A Study of Magnetic Resonance and Ultrasound based Through-the-body Communications

Rajpreet K Gulati Walia, Hirsa Kia, Krishna Kant
Temple University, Philadelphia, PA 19122, USA

***Abstract*—In this paper we study the performance of through-the-body communications for both on-body and in-body nodes using both Magnetic Resonance Coupling (MRC) and Ultrasound Coupling (USC). We do this in the frequency range of tens of MHz or lower, where the specific absorption rate (SAR) of EM signal in the body is expected to be very small and longer distance communications are possible with small antennas. The key problem addressed here is simulation modeling of the MRC/USC communications using the Sim4Life simulator along with its detail virtual population (ViP) phantom models, and compare them against direct on-body measurements. The results show a very close match in most cases, which lends confidence in the measurements, and the quality of EM propagation and human phantom models in Sim4Life. The results also reveal some peculiar characteristics of MRC transmission through the body, such as the notion of optimal frequency depending various antenna parameters. Overall, we find that both MRC and USC can easily reach several 10s of cm with only 1mW of transmitted power.**

***Index Terms*—Magnetic Resonance Coupling; Ultrasonic Coupling; intra-body network; wireless power transfer, Sim4Life, path-loss.**

I. Introduction

There is an increasing array of human assistive technologies that generally require sensing some vital parameters and accordingly applying or simply recommending some corrective action. The action could be mechanical force (e.g., inflation, pressure, etc.), electric field (nerve or muscle stimulation), chemical (e.g., drug delivery), etc. [1], [2]. The signal may not necessarily be captured in the same place where the action occurs; for example, sensors monitoring the foot movement may require control at the knee to maintain stability. Often, the signals must be collected from multiple points on or inside the body, thereby requiring a small wireless network that can collect all signals efficiently without interference, fuse them together, and decide upon the appropriate action. Such networks are crucial for managing chronic conditions and may include some sensors attached to the skin while others are implanted. For example, bladder control is a common problem in older people and proper bladder management may require tapping signals in multiple places including muscles (Detrusor muscle that allows storage, and Sphincter that controls opening/closing of bladder outlet), efferent nerves from the spinal cord (Pelvic, Physogastric, and Pudendal that command those muscles), the corresponding afferent nerves for feedback to the spinal cord [3], and perhaps direct measurement of the pressure (fullness) in the bladder itself [4]. It is expected that all these signals would be routed to a "hub" node that analyzes them and controls the electric field or drug delivery. The control functionality may reside in an on-body node for better control (possibility of more energy and hence computing capability, easier troubleshooting, more flexible operation, etc.) Even if the control node is implanted, an on-body node is generally required for electrical stimulation [3], [5], because of its significant power requirements.

Thus, through-the-body wireless communications (TBWC) become essential to operate these networks, but TBWC faces several challenges. The first problem is powering the nodes. Since the implants must be as small as possible to avoid tissue damage, long-lasting batteries are ruled out due to their large size. Instead, it is highly desirable to employ wireless power transfer (WPT) to the nodes. The node could then use a small supercapacitor to hold the required charge for relatively short periods of time. The energy to be transmitted could be either harvested at other in-body/on-body nodes (e.g., close to the heart or lungs) or supplied from a battery-operated on-body device such as a smart watch. An efficient WPT mechanism is crucial to ensure that the nodes can receive adequate energy supply. Note that even a small 20db path-loss through the body would reduce 1 mW transmitted power to only 10μW on the receiver side. Put another way, 99% of the transmitted power will be wasted or absorbed by the tissue.

Another difficulty with TBWC is that normal RF communications do not work due to water-rich intrabody environment [6], [7]. In particular, the transmission from the ubiquitous short-range RF technology such as BlueTooth Low Energy (BLE) operating at 2.4 GHz is largely absorbed or diffracted by complex tissue geometries and highly variable electric permittivity inside the body [8]. These characteristics imply both the need for higher power and potential safety issues of persistent exposure. BLE also suffers from shadowing effects from the body parts; for example, it is reported in [9] that the head causes a 40dB attenuation in ear-to-ear BLE channel. Since RF propagates well through the air, its use inside the body also brings about security issues, i.e., the possibility of eavesdropping, intrusion, or jamming by adversaries.

Thus, an appropriate Human Body Communications (HBC) technology is needed that requires low power, small antennas/transceivers, and conforms to the medical safety issues. Several HBC technologies have been studied in the literature, including Galvanic coupling, Capacitive coupling, Magnetic Resonance Coupling (MRC), and Ultrasonic coupling (USC). Overviews of these may be found in our earlier work [10] and elsewhere [11]. These technologies have been amply discussed

in the literature; for example, see the overview in [12], [13]. Our experiments in [14], [15] show that among the electromagnetic methods, MRC works much better than Galvanic or capacitive coupling. It is also very robust against variations that one would expect in on/in-body environment such as movement, posture, clothing, person to person variations (e.g., build, weight, etc.) [15]. We have also studied Ultrasonic Coupling (USC) and compared it against MRC in [10]. We find that USC works quite well and often better than MRC in lower frequency range, but in the higher frequency range it is difficult to design a USC transducer since the diaphragm thickness goes down with frequency [16]. Also, USC antennas have been reported to be very sensitive to misalignments [17] and require proper acoustic impedance matching [18]. Thus this paper explores MRC in a bit more depth than USC.

Both MRC and USC have been explored in the context of both wearables (on-body) and medical uses (on/in-body) both for communication [8], [19] and WPT [20]. For example, ref [8] considers ear to ear transmission with 2cm air gap on each side, whereas our goal in this study is to consider a truly on-body/in-body with no air-gap as far as possible. The biomedical application of MRC and USC generally consider very short distances (a few mm to few cm). Ref [21] explores an USC powered microprobe for electrolyte ablation. Ref [22] develops a USC power receiver for medical devices. Ref [22] discusses MRC power transfer to medical devices. Ref [23] designs a sub-10-pJ/bit 5-Mb/s MRC transceiver.

There are currently very few detailed studies of MRC/USC propagation through the body at frequencies of a few to few 10's of MHz range and distances of tens of cm. Much of the longer-range characterization models the body either separately for different types of tissues, or by using average dielectric properties, or in the context of very high frequencies. Ref [17], for example, explores both through COMSOL simulation of EM propagation through a homogeneous soft-tissue media and via some experiments on chicken breast. Ref [8] is typical of channel characterization efforts through measurements and simulations. It considers propagation over much higher frequency region (50Mhz to 2.4GHz) and uses average dielectric properties of human body, which is not appropriate at lower frequencies. Several other studies use simplified simulation models such as [13]. Our study concerns longer distances that can go to tens of cm.

The purpose of this paper is to report the comparison between measurement and simulation results for MRC, and to a lesser extent USC. Since conducting in-vivo measurement experiments for implanted nodes is largely infeasible, the actual experiments are limited to on-body scenarios. Instead, we used detailed simulations to explore the performance of MRC and USC communications both for on-body and in-body scenarios. Such simulations must accurately model both the intrabody environment and the propagation of signals through it. For this, we have used the Sim4Life simulation package [24] which provides the capability to model electromagnetic propagation through extremely detailed and high-fidelity human body phantoms called the Virtual Population (ViP) models.

The results suggest several interesting and not necessarily expected conclusions about the MRC and USC communications through the human body. First, and most significant, is the fact that the transmission of these signals through the body is completely different than what would be expected in a homogeneous nonconducting media such as air. Second, the simulation and measurement results for on-body communication agree quite closely in all cases, with the difference limited to at most a few db. This suggests a high accuracy of both the Sim4Life EM propagation modeling and that of the ViP models used by the simulations. Third, the simulations show that the difference between placing the antenna on-body (i.e., on skin) vs. in-body (under the skin and fat-layer) is quite small. This further suggests that the results obtained via simulation for intrabody scenarios provide a good approximation of what might be expected in real measurements. We discuss these results in detail to provide insights into how MRC and USC communications might behave for TBWC.

The rest of the paper is organized as follows. In section II we discuss the magnetic and Ultrasonic Coupling basics. Section III discusses our detailed experimental setup. The systematic comparison of magnetic and ultrasonic coupling through the human body is discussed in section IV. The paper is concluded in section V.

II. MRC and USC Communications

A. Magnetic Resonance Coupling (MRC)

MRC involves resonant communication between two coils as illustrated in Fig. 1. Each coil is in series with a capacitor to create a LC tank that has resonance frequency of $f_r = 1/(2\pi\sqrt{LC})$ where L and C are the inductance of coil and the capacitance of the capacitor respectively. For maximum energy transfer efficiency, the transmitter and receiver sides must have matching resonance frequency. Furthermore, to avoid reflections, the two sides also need to have matched impedance (which is purely resistive at resonance frequency).

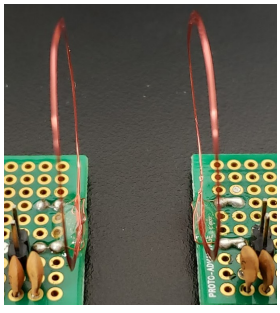

Fig. 1. Illustration of MRC

The inductive energy transfer between a transmit and receive coil can be used both for wireless power transfer (WPT) and communications, and the two can occur simultaneously. The communication requires a suitable modulation technique, for which we have used simple BPSK, since the focus of this work is not on high data rates. In the on-body TBWC use case, the coils are placed on the skin with an electrical gel to avoid any air-gap (and shielded on top to avoid through the air communication). For intra-body use, the entire circuitry including the LC antenna would need to be enclosed in a bio-compatible, non-conducting, and non-magnetic substance. This would effectively add a gap between the coil and the tissue and poses some impedance matching issues that we have not accounted for.

An important performance indicators such circuits is the *quality factor* Q, defined as the ratio of the energy stored in the circuit to the energy dissipated by the circuit [25], and is given by $Q = 1/(2\pi f_r RC)$ where R is the resistance of the circuit. The quality factor is also defined as the frequency-to-bandwidth ratio of the resonator, i.e. $Q = f_r/\Delta f_r$ where Δf_r is the resonance width, i.e. the bandwidth over which the power is greater than half the power at the resonant frequency. For series RLC circuit shown in Fig. 2, the Q factor is given by $(1/R)\sqrt{(L/C)}$ and is inversely proportional to the circuit resistance R. The Q factor defines how "peaky" the resonance is; a high Q-factor is desirable for efficient energy transfer, but the resulting peakiness also means that a slight drift in R, L, or C components would reduce the efficiency drastically. The drift can occur due to a variety of reasons including environmental (e.g., temperature), component drift, circuit/enclosure issues, and the variations in the effective body capacitance that contributes to the resonance frequency.

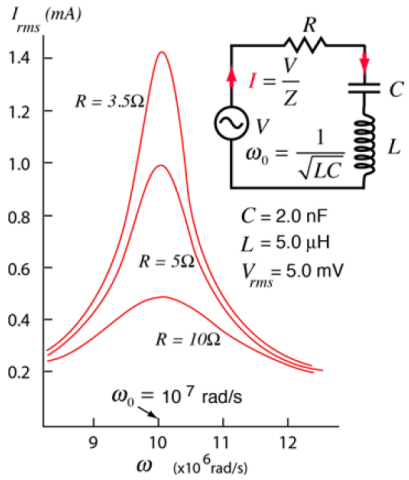

Fig. 2. Illustration of Q factor in MRC

An obvious question regarding the use of MRC for WPT/communications is their impact on the body tissue. Extensive studies on tissue exposure exist for frequencies *above* 5MHz [26], [27]. International bodies, such as the International Commission on Non-Ionizing Radiation Protection (ICNIRP) and the Institute of Electrical and Electronics Engineering (IEEE), have provided basic restrictions in terms of, first, the peak spatial specific absorption rate over any 1 or 10 g of tissues to prevent tissue heating in the frequency range from 100 kHz to 10 GHz and, second, the induced electric field averaged over a volume of tissue to prevent nerve stimulation below 10 MHz. To ensure user safety, the peak average SAR should not exceed the limits of 1.6 and 2 W/kg, imposed by the IEEE over 1 and 10 g of tissues, respectively. In this study, 1 g SAR is considered, which is more restricted compared to the 10 g SAR limit. Given the extremely low power and currents (1 mW/ 1 mA), at a low voltages in real applications, SAR is of no concern below 100KHz [28]–[30].

B. Far-field vs. Near-field Energy Transfer

Magnetic resonance based energy transfer has a very long history, and is popularly used in wireless charging of phones and other devices, and recently there have been many studies for its use in underwater communications [31], underground communications [32], body area networks [33], and biomedical applications [34], [35]. We have also studied this technology in our earlier work [36]. In all these contexts, it is assumed that the technology works in the *near-field* regime, often under the name NFMI (near field magnetic induction). In contrast, the traditional RF communications such as BLE are considered as *far field*. The difference is the communications distance, say d, as compared to the carrier wavelength λ_r. For example, at 2.4 GHz, the free space (or in-Air) wavelength λ_r is only 12.5cm, which is much smaller than the distances that BLE is intended for (several meters to 10s of meters). In case of far field, the RF power is transferred through Friis equation for propagating EM waves. The key characteristic of far field operation is the intimate coupling between the electric and magnetic fields through Faraday's and Ampere's laws which leads to propagating waves. Near-field refers to the opposite situation which holds for operating distances substantially less than the wavelength. For example, a popular operational frequency for NFMI is 13.56MHz, which is the standard frequency for RFID operation. At this frequency, the free space wavelength λ_r is 22m; thus, communications within 2-3m could be considered as near-field. More precisely, the near-field threshold is given by $\lambda_r/2\pi$ [37], or 3.5m at 13.56MHz.

The concept of near-field is really an idealization and characterized by making some assumptions in applying Maxwell's equations for EM propagation. In the *electro-static* near-field approximation, we ignore the contribution of varying magnetic field on the electric field (i.e., in Faraday's Law) whereas in the *magneto-static* near-field approximation, we ignore the contribution of varying electric field on the magnetic field (i.e., in Ampere's Law). The resonant LC circuits in MRC produce a strong magnetic field and thus magneto-static is the appropriate approximation since the contribution of electric charge to magnetic field can be ignored. The capacitive coupling mentioned above generates a strong electric field and thus can be characterized as quasi electro-static over short distances. The near-field approximations decouple the electric and magnetic field and thus can be assumed to be "instantaneous" (since there is no time derivative in the approximated Maxwell's equations) rather than propagating. This not only simplifies solution to the equations but also field that is largely not radiative.

C. Near-Field MRC Transmission in Air

Under near-field assumption, we can relate the induced current in the receive coil (denoted I_2) to that in the transmit coil (denoted I_1) in terms of the mutual inductance between the two coils (denoted M) and the coil parameters. In particular,

$$I_2 = -\frac{j\omega_r M}{R_2} I_1 \tag{1}$$

The mutual inductance M can be expressed in terms of the *coupling coefficient* k, and the inductances of transmit and receive coils, denoted L_1 and L_2 respectively. That is, $k = \frac{M}{\sqrt{L_1 L_2}}$. Thus if P_1 and P_2 are the transmitted and received power respectively, the power transfer ratio is given by [25]

$$\frac{P_2}{P_1} = \frac{\omega_r^2 M^2 R_1 R_2}{R_1^2 R_2^2} = \kappa^2 Q_1.Q_2 \tag{2}$$

where Q_1 and Q_2 are the quality factors of the transmit and receive coils respectively. Thus, the power transfer is

proportional to the coupling coefficient and the quality factors of the transceiver coils.

It is possible to characterize M (or κ) explicitly in terms of coil diameters (denoted ρ_1 and ρ_2 for transmit and receive coils), number of turns in those coils (K_1 and K_2 respectively), distance h between the coil centers, and the relative orientation of the plane of the receive coil relative to that of the transmit coil (denoted by angles β_1 and β_2 in the two dimensions). The derivations (for free space) are widely available [38]–[40] and reported in [37]. The key assumption in this derivation is that $h \gg \max(\rho_1, \rho_2)$, i.e., the distance between coils is large enough that the coil geometry does not matter much. Then, using Lenz's law, the induced AC current in the receiver coil is proportional to the rate of change of the magnetic flux according $I_r \propto M_{t\to r} f_r$ where f_r is the resonance frequency. Thus

$$I_r \approx f_r \frac{\mu\pi K_t K_r \rho_t^2 \rho_r^2}{2h^3} \left| \cos\beta_t \cos\beta_r - \frac{1}{2}\sin\beta_t \sin\beta_r \right| \quad (3)$$

This equation suggests the following: The induced current increases linearly with the operating frequency and goes down very rapidly with distance r (as r^{-3}). Since the power is proportional to I_r^2, the induced power decays as r^{-6}, which is much faster than the decay for far-field (or RF) case, where the power goes down as r^{-2} with distance r. The very rapid decay of the induced power with distance makes the MI technology inherently a small range technology, and this effect is usually more limiting than the near field requirement of $r < \lambda_r/(2\pi)$. The area of transmit and receive coils (proportional to ρ_t^2 and ρ_r^2 respectively) and the number of turns (K_t and K_r) directly influence the mutual inductance and hence the induced current. Increasing the range requires bigger coils and more turns, both of which may be undesirable in applications where small size is required. The frequency and the transmit coil current directly increase the induced current, and hence the overall power consumption (bad) and the range (good).

D. MRC Transmission in Other Media

For transmission through materials other than air, it is important to consider their electrical and magnetic properties, which affect the speed of EM propagation ("speed of light"). The latter, denoted c_r is given by:

$$c_r = 1/\sqrt{\epsilon \times \mu} \quad (4)$$

where $\epsilon = \epsilon_r \epsilon_0$ is the electrical permittivity and $\mu = \mu_r \mu_0$ is the magnetic permeability of the media with ϵ_r, μ_r being values relative to that of the air with permittivity ($\epsilon_0 = 8.85410^{-12}$), and permeability $\mu_0 = 4\pi \times 10^{-7}$. Since $c_r = \lambda_r \times f$, a high permittivity or permeability reduces both λ_r and c at a given frequency. For the human body $\mu_r \approx 1$ ϵ_r varies tremendously from organ to organ [41], [42] with absolute values (including real and imaginary parts) ranging from tens to thousands. The imaginary part results from the conductivity of various organs, which also varies significantly. Furthermore, the permittivity is not constant but goes down with the operating frequency.

Fig. 3 show a sample of permittivity and conductivity at both 13.56 MHz and 25 MHz and one can see significant

	13.56Mhz		25.0 MHz	
Tissue type	Relative Permittivity	Elec. Cond. (S/m)	Relative Permittivity	Elec. Cond.
Blood	210.6	1.12	133.1	1.15
Bone (Cancellous)	59.3	0.13	43.5	0.14
Bone (Cortical)	30.6	0.05	22.5	0.05
Brain (Grey Matter)	263.4	0.33	172.7	0.40
Brain (White Matter)	153.1	0.18	111.3	0.22
Breast Fat	7.2	0.03	6.3	0.03
Esophagus (stomach)	189.3	0.80	124.6	0.83
Fat (avg.)	25.4	0.06	18.6	0.06
Large Intestine	217.1	0.51	146.9	0.56
Lung (inflated)	95.4	0.24	60.8	0.26
Muscle	138.4	0.63	99.3	0.65
Skin (dry condition)	285.2	0.24	175.7	0.32
Small Intestine	362.7	1.39	215.3	1.47

Fig. 3. Electrical Properties of Human Tissue

variations even within a single organ. Thus the near-field limit inside the body (and hence the validity range of quasi-static assumption) is much smaller than in air. For example, at 13.56MHz, the near field limit for muscle is only about 30cm. Thus, for communication/energy-transfer distances of more than 30cm inside the body, the transmission operates in "mid-field" where we have both near-field and far-field effects, and can be quite complex. At 25 MHz, the limit shrinks to 16.2cm, and thus the propagation would be mid-field in many practical intrabody network scenarios. Perhaps because of these factors, the propagation of MRC within the body shows quite a different behavior than predicted by equations above, and we explore this aspect both via measurement and simulation in this paper.

E. Characteristics of Ultrasound Communications

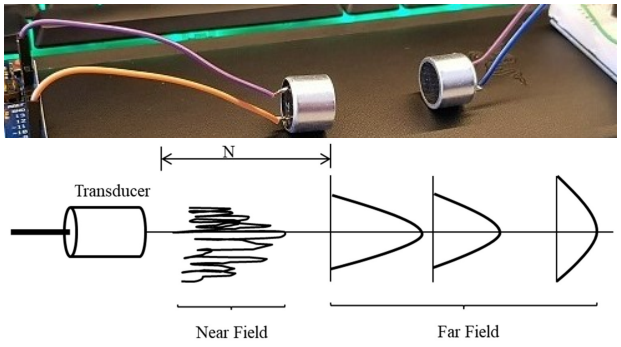

Fig. 4. Ultrasonic Coupling Characteristics

USC is a very well-researched technology [43] and has been widely used in various clinical applications [44], and specifically explored for both communications [45] and power transfer [17], [46]. USC is very popular for imaging in the human body, with typical frequencies ranging from a few 100 KHz to a few MHz, although it is possible design transducers for wider ranges as well. The USC velocity in human tissue is around 1500 m/s. Thus at 1 MHz, the wavelength λ is only 1.5 mm, and even lower at higher frequencies. Small USC devices

have been used extensively in implants without any reported side effects, and provide a range of 5-10 cm communication range.

Ultrasound propagates via pressure waves from a transducer in form of a vibrating diaphragm interfaced with a piezoelectric crystal for electrical to ultrasound conversion on the transmit side. A reverse process occurs on the receive side. The intensity I of USC waves (in mW/cm^2) can be related to the pressure P, the density of the media ρ, and the speed of sound c as $I = P^2/(\rho c)$. FDA regulates this intensity to be 720 mW/cm^2 for most of applications [47], [48]. Fig. 4(a) shows USC communication in air using two cylindrical transducers with a vibrating diaphragm.

As with MRC, USC also shows the near-field and far-field effects which are well characterized through homogeneous media such as air or water. In the near-field region, the pressure waves are irregular but focused, i.e., in the shape of a cylinder along the transducer axis (see Fig. 4(b)). The extent of near-field, denoted as N in Fig. 4(b), is given by $N = D^2/(4\lambda)$. Thus for a transducer diameter of 1cm and $\lambda = 1.5mm$, $N = 16.7$mm. This is the range for which USC has typically been used in biomedical applications and thus will be expected to suffer very little attenuation. Beyond this range, into the far-field range, the diameter of the pressure wave expands exponentially, which means that the pressure drops accordingly. In particular, the pressure $P(d)$ at distance d is given by $P(d) = P_0 e^{-af^b d}$ where a and b are some positive constants and f is the frequency. Also, since USC waves are mechanical, they scatter at boundaries between two materials (e.g., soft tissue and bone), according to Snell's law. With many boundaries of irregular shape in the body, the net impact of the scattering on the magnitude of the signal can be described statistically using the Nakagami distribution [49]. It is shown in [45] that the noise in the tissue environment $\mathbb{N}(f)$ (with f in KHz) can be approximated as $log\mathbb{N}(f) = -15 + 20\ log(f)$. Thus, as f increases, the noise also increases and the signal attenuates rapidly. This suggests a rather short tissue penetration of USC. However, our experimental and simulation results suggest that USC works quite well inside the body – in fact, even better than MRC.

USC performance in an on-body scenario may be enhanced by the phenomenon of Rayleigh surface acoustic waves (SAW) [50]. Surface acoustic waves travel along smooth surfaces and can cover significant distance without much attenuation; however, undulations in the surfaces of the order of a few wavelengths can disrupt them. For on-body applications, we have both scenarios, e.g., bare skin (typically quite smooth) and skin covered with clothing or other materials. SAW should not play a significant role inside the body.

III. Experimental and Simulation Setups

A. Real Measurements

In our prior work, we have extensively evaluated MRC experimentally in on-body scenario [14], [15] and we only briefly summarize the setup. We used flat circular coil that can be placed securely on the skin with an electric gel to make good contact (see Fig. 5). The coils were shielded magnetically on the top so that there is no signal leakage into the air. The transmit and receive coils were identical and placed on different part of a volunteer's body. We used coils of several different sizes, although most of the results reported here were obtained using a 20 mm diameter case.

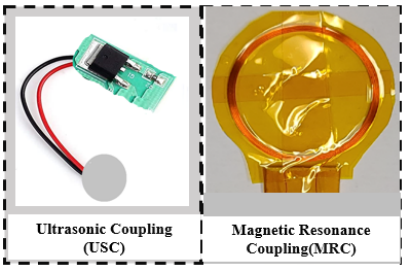

Fig. 5. MRC and USC Antennas used in experiments

For the experiments in this paper, we needed the capability to design antennas that can operate on any desired frequency (in 1-50 MHz range). However, there are several practical problems in doing this. A simple solution is to use mechanically variable inductors and capacitors (usually changed by turning a screw), but these were found to be quite unstable and not usable. A more sophisticated method is to use voltage controlled inductors and/or current controlled capacitors, but these too were not very stable. Therefore, we built LC circuits with suitably chosen capacitors values along with change in the number of turns to change the inductance. (Changing coil diameter is requires different coils which were not available.) Note that the resistors and capacitors come only in certain well-known sizes and have 1% or worse tolerance; therefore, achieving the precise resonance frequency or matching the transmitter and receiver is often difficult even to start with. We largely achieved this by trial and error, and it is a very time consuming process.

There are other challenges also brought about by using the antenna on-body. Human body has a small capacitance that must be accounted for in achieving the precise resonance frequency. Other issues concern the quality of antenna contact with the skin and the skin properties of the person. For example, skin moisture and resistance is a function of when the person took shower, humidity, temperature, stress level, mood, etc. Thus the path-loss results can easily vary by a few db or more across experiments for same distance and frequency on the same person.

For all the experiments, the volunteer did not stand on bare ground as that would create ground path between the transmitter and receiver. Instead, the volunteer was either seated or standing on non-conducting floor, and we confirmed that different postures (e.g., seated on cushioned chair with feet off the ground) did not make any difference. We measured the communication performance in two ways. First, we connected the transmitter to a signal generator and receiver to vector network analyzer (VNA) to measure the received signal. There was no common ground connection between the signal generator and the VNA, as that would invalidate the results. This method only provides

us with the path-loss.

For real packet transmissions, we used a pair of USRP (Universal Software Radio Peripheral) N210 boards produced by Ettus Research (https://www.ettus.com/all-products/un210-kit/). The boards enable flexible implementation of software radio including various type of modulation schemes along with the ability to connect different types of antennas. It includes a Xilinx® Spartan® 3A-DSP 3400 FPGA, 100 MS/s dual ADC, 400 MS/s dual DAC and Gigabit Ethernet connectivity to stream data to and from host processors. A modular design allows the USRP N210 to operate from DC to 6 GHz. In our experiments, we used BPSK modulation to study packet delivery ratio through the body at different distances.

B. Simulation Based Evaluation

As discussed earlier, real experiments must be limited to on-body case, and even in that scenario are inconvenient to perform on a large scale. This gap can be easily filled with a comprehensive simulator that supports standard methods to solve Maxwell's equations in a complex environment. Equally important is the availability of highly detailed and realistic human phantom models. There are several open source packages summarized in [51], plus two commercial packages COMSOL (https://www.comsol.com/), and Sim4life [24]. Unfortunately, most do not come with human phantom models. Two packages that do include them are CST studio (open source) and Sim4Life (non open-source). We have used Sim4Life in this work, and it supports extremely detailed and accurate "Virtual Population" (ViP) models. For the modeling of the propagation of pressure waves through extremely nonhomogeneous media such as tissue and bone, Sim4Life provides a full-wave Acoustics Solver called P-ACOUSTICS. This solver is based on the linear pressure wave equation and is tuned for heterogeneous, lossy materials. This approach is capable for all of the simulation like scattering, reflection, refraction, diffraction, interference, and absorption. We have used this approach for solving path loss in ultrasonic transducer.

Realistic modeling of EM propagation through the human body requires accurate handling of surfaces with very different EM properties; therefore, numerical solution using a fine 3D grid ("voxel") is necessary. The three main methods in this regard are [51]: Finite-differences-time domain (FDTD), Finite Element Method (FEM), Method of Moments (MoM), or equivalently, Boundary Element Method (BEM). We have used the FDTD method in our modeling using full Maxwell's equations (i.e., not magnetostatic assumption) and thus the results should be valid regardless of the frequency. However, to avoid error accumulation due to finite differences, the voxels must be rather small in size.

An MRI-based full-body voxel model, the Duke, obtained from a virtual population was used. The model was segmented into about 80 anatomical body tissues/organs, with a resolution of 1.5 × 1.5 × 1.5 mm throughout the body. The height and weight of the model were 1.77 m and 70.2 kg, respectively. Since a FEM solver is capable of operating at MHz frequencies (fr= 50 MHz), we obtained the path loss distribution around the MRC/USC system with the human body model using the magneto FEM vector-potential and ultrasonic FEM solver. For USC, we used a parabolic diaphragm with specific focal point.

IV. Results and Discussion

A. Experimental MRC and USC Results

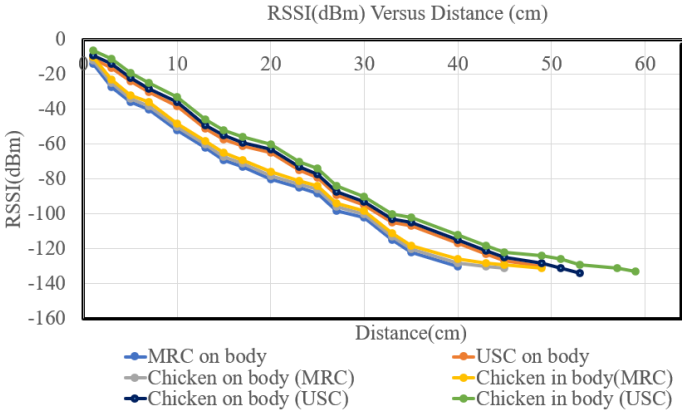

Fig. 6. MRC and USC RSSI Comparison at 8MHz

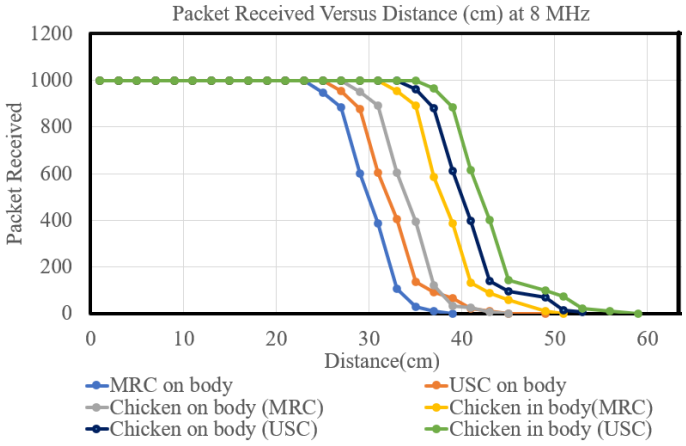

Fig. 7. MRC and USC PDR Comparison at 8MHz

Fig. 6 shows the RSSI (received signal strength indicator) and Fig. 7 shows the PDR (packet delivery ratio) for both MRC and USC at the same frequency. For USC, we used a 20mm diameter disc transducer whose thickness must decrease with the frequency as shown in Fig. 5. We chose it as 8MHz here since USC transducers at higher frequencies were not available. Also note that because of the fundamental differences between MRC and USC, a 13.56 MHz frequency for USC is not necessarily meaningful.

To enable in-body experiments, we have also included experiments on grocery-bought chickens (multiple of them jammed together for longer distances). It appears that USC results in about 10db advantage over MRC and thus shows a slightly longer range. It is also seen that the in-body case provides somewhat better performance in all cases than on-body, possibly due to loss at the antenna-skin interface. Finally,

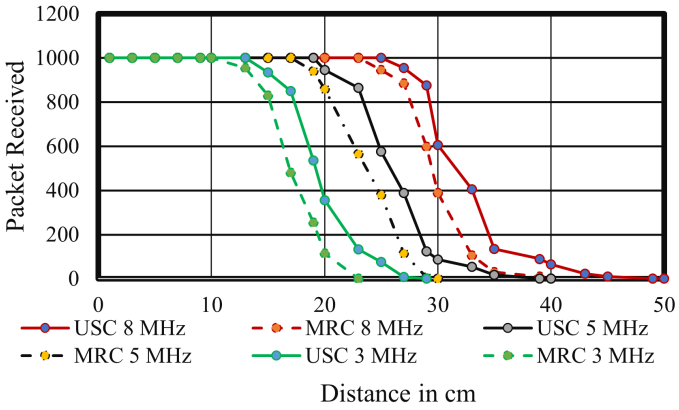

Fig. 8. MRC and USC Comparison at 3, 5, and 8 MHz

the range is seen to be a bit more than 30 cm in this case. Fig 8 shows the PDR at 3 different frequencies of 3, 5, and 8 MHz. It is seen that in this low frequency range, USC consistently performs better than MRC. (As seen later, this trend is not maintained at higher frequencies).

B. Comparison of Measurement and Simulation Results

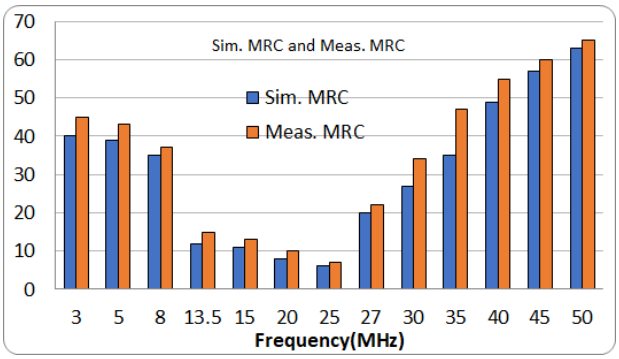

Fig. 9. MRC measured vs. simulated Path loss a a function of Frequency

We next ran Sim4Life for several situations conditions similar to those for real measurements. Note that the duke phantom model in Sim4Life does not directly represent the characteristics of any of the volunteers and thus achieving the same path length through the body and the same positions on the body is not possible. Nevertheless, our extensive measurements in [15] indicate that the differences should not be significant. Fig. 9 shows the comparison for a wide range of frequencies from 3 MHz to 50 MHz. It is seen that in most cases, there is a very good match between the two. In all cases, the measured loss is larger than the simulated one which could be explained by the fact that the simulated situation is ideal – there is no issue of skin-contact quality, field leakage outside the body (since none is modeled), or even the minor loss of signal between the measuring equipment and the measured signal on the body. Accounting for this, will perhaps show an even better match. We found such a match in all the other (unreported) cases as well. The somewhat variable difference between measured

TABLE I
SIMULATION VS. MEASUREMENT AT 13.56 MHZ

TX position	RX position	Dist. (cm)	PL(USC) Sim	PL(USC) Meas	PL(MRC) Sim	PL(MRC) Meas
Right lower Calf	Left Lower Calf	15cm	12	14	9	11
Right upper Calf	Right upper Calf	20cm	14	15	12	13
Right Waist	Left Waist	36 cm	17	21	12	14

TABLE II
SIMULATION VS. MEASUREMENT AT 20 CM DISTANCE AND VARYING FREQUENCIES

Freq(MHz)	Sim(USC)	Meas(USC)	Sim(MRC)	Meas(MRC)
8	32	35	39	37
5	35	39	38	43
3	37	40	39	45

and simulated values can be attributed to various sources of variations including: (a) body-type of the volunteer vs. that of the phantom, and (b) difficulties and practical issues in setting the precise values of L and C in each case, as mentioned in section III-A.

A consistently good match provides us some assurance on three fronts: (a) the quality of FDTD simulation in Sim4Life in terms of handling the very complex environment, (b) the quality of ViP body models both in terms of anatomy and the electromagnetic properties of various organs, and (c) the accuracy of experiments that can easily be affected due to parasitic capacitances and unknown ground paths. The most interesting result from Fig. 9 is the "sweet-spot" for the frequency even in a rather limited range of 2-50MHz. In the figure, the path-loss is minimum around 25MHz and increases on both sides. The model in section II-C for propagation through the air cannot explain such a behavior. We believe that this is a result of frequency dependent permittivity and conductivity as illustrated in Fig. 3. The frequency at which the minimum occurs on several parameters as discussed later, and should not be construed as fixed. Even more significant, the actual values of path-loss very much depend on the Q-factor of the coils. In Fig. 9, the Q-factor is quite high (210 at 25 MHz), which is unrealistic for long term operation as discussed in section II-A. If we bring Q down to a more reasonable 100 or lower, the path-loss would likely increase by another 10-15db. Another issue is that the Q-factor will change with frequency because of practical difficulties in maintaining the same L/C ratio. However, the experiments do suggest that the behavior remains intact.

Next we report results from a few experiments and corresponding simulations, performed using both USC and MRC. We chose three different parts of the body: 1. Right-lower Calf to Left-Lower Calf (15cm), 2. Right-upper Calf to Right-upper Calf (20cm), and 3. Right Waist to Left Waist (36 cm). The results are shown in Table I.

As expected, the measured path-loss is somewhat higher than the simulated value, but they are quite close. Next, we show

simulation vs. measurement for MRC and USC at 3, 5, and 8 MHz frequencies and the distance fixed at 20cm, as shown in Table II. These results again show a good tracking of simulation vs. measured results for both MRC and USC. It is also seen that USC performs better than MRC at lower frequencies as observed earlier. Also, as expected, as stated before, the path-loss goes down with frequency in this low frequency range. For USC, this behavior is contrary to the equations discussed in section II-E, where the pressure at a given distance supposed to go down exponentially with the frequency. For MRC, the range should increase with the frequency, since higher frequency implies higher energy. However, the in-air behavior of power going down as sixth power of distance (see section II-C) clearly does not hold. A higher water content in the body might be helping ultrasonic waves to achieve more extended range. However, further exploration of physics is necessary to substantiate this claim.

C. Further Simulation Studies of MRC

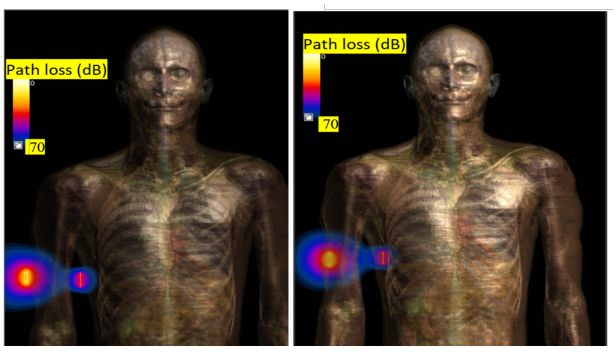

Fig. 10. MRC Signal Strength Plots for in-body and on-body simulations

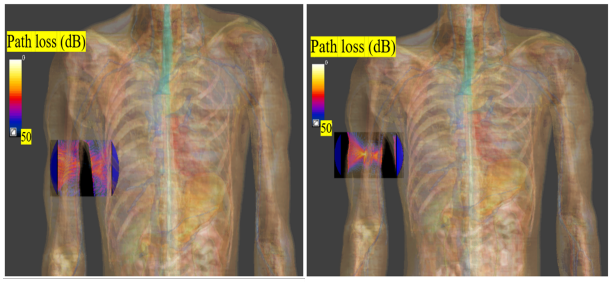

Fig. 11. USC Signal Strength Plots for in-body and on-body simulations

Having obtained some confidence on the simulation results, we conducted more extensive simulation experiments, largely focusing on MRC. In particular, we explored the potential difference between in-body vs. on-body placement of the antenna. Fig. 10 shows the antenna placements for MRC and the plot of magnetic field, with blue indicating weak field and red the strong field. Fig. 10 shows the pressure density for USC using a parabolic antenna.

Fig. 12 shows the comparison of in-body vs. on-body results. It is seen that the MRC path loss is higher for frequencies up to about 10 MHz, and beyond that the difference between the two very small; in fact, at the typical MRC frequency of 13.56MHz, MRC has slightly lower loss, and at higher frequencies the difference is negligible. Recall that the optimal frequency point for MRC is closer to 25 MHz, at which it is difficult to get USC transducers. This is the reason we largely focus on MRC. It is also seen that the difference between on-body and in-body scenarios is rather small, with on-body showing a slightly higher path-loss.

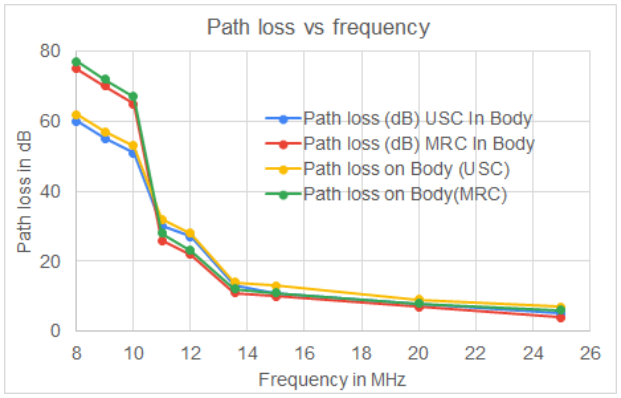

Fig. 12. MRC and USC simulation result for in-body and on-body cases

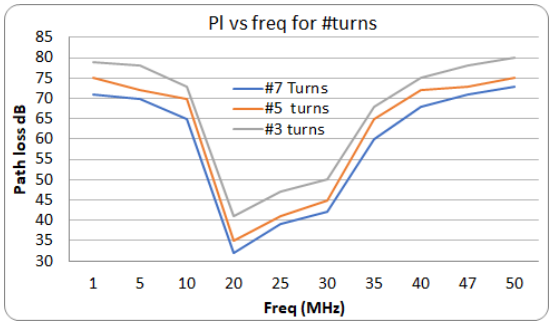

Fig. 13. Simulated Path loss vs frequency with different #turns in coil

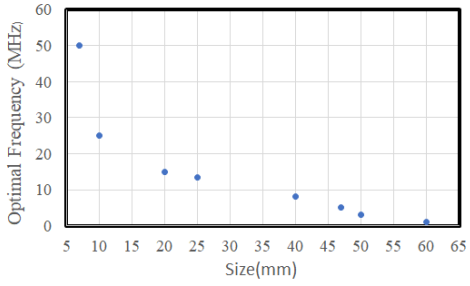

Fig. 14. Optimal Frequency of Operation vs. coil diameter for 7-turn coil

We further studied the behavior of MRC with frequency when the number of turns of the coil are changed. Fig. 13 shows the behavior of 20mm coil for 3, 5, and 7 turns. The

results are generally expected – the path-loss decreases with the number of turns. One thing not obvious is slight shift to the left with increasing number of turns. This behavior has been reported in [52] and is again not expected in a homogeneous media like air.

Given the "sweet-spot" behavior of path-loss vs. frequency, we decided to examine optimal frequency as a function of coil size for MRC. The result is shown in Fig. 14. It is seen that there is a consistent decrease in optimal frequency as the coil size increases. Please note that these results were obtained by trial-and-error, since there is no equation to indicate the optimal operating point, therefore, the results are approximate. Further approximation errors can be expected due to variation in the Q-factor. To keep the same Q-value, the ratio of L to C would need to be maintained the same; however, this is difficult to do as explained in section III-A.

Our exploration suggests that the signal propagation behavior through the human body is quite different than in a homogeneous nonconducting media like air. The results are also markedly different than are often observed with idealized modeling of body with average dielectric parameters or by considering tissues of only one type. Our results are, however, consistent with those reported in [52] and [53]. Other researchers have also reported variations in channel gain as a function of frequency for both MRC and uSC [8], [17]. However, the complexity of the body and different frequency ranges, dielectric property assumptions, etc. make a direct comparison difficult.

V. Conclusions

In this paper we have examined in detail the characterization of magnetic resonance and ultrasound based communications through the human body, both via direct on-body measurements and via simulations using the Sim4Life package and ViP phantom human body models. We show a close match between measured and simulated results in spite of many limitations of the measurements, which provides confidence in measured results and SIm4Life simulations. The most significant result from these measurements is that the human body does not behave at all like a homogeneous, nonconducting media like air, and thus the mathematical equations expressing the behavior in homogeneous media cannot be used to characterize the behavior through the body. The simulations and measurements provide many non-intuitive results that are difficult to explain and somewhat surprising. For example, the path-loss as a function of frequency shows a unimodal behavior, with minimum loss at a frequency that is determined by the coil size and number of turns. In the future we will explore such behavior further to understand the reasons and the impact of various factors that are difficult to control in practice.

Acknowledgements

The project was supported by the National Science Foundation (NSF) grants CNS-2129659. The authors would also like the help from and discussion with Sayemul Islam (Temple University), Izaz Ali (Hanyang University, Korea), and Dr. Amitangshu Pal (IIT, Kanpur, India).

References

[1] A. Mendez *et al.*, "Estimation of bladder volume from afferent neural activity," *IEEE Transactions on Neural Systems and Rehabilitation Engineering*, vol. 21, pp. 704–715, 2013.

[2] K. Kaszala *et al.*, "Device sensing: sensors and algorithms for pacemakers and implantable cardioverter defibrillators," *Circulation*, vol. 122, pp. 1328–1340, 2010.

[3] S.-Y. Lee *et al.*, "Bladder control implants," in *Handbook of Biochips: Integrated Circuits and Systems for Biology and Medicine*. Springer, 2022, pp. 3–20.

[4] E. T. Roche, "Implanted device enables responsive bladder control," 2019.

[5] F. Stewart *et al.*, "Electrical stimulation with non-implanted electrodes for overactive bladder in adults," *Cochrane Database of Systematic Reviews*, 2016.

[6] D. Werber *et al.*, "Investigation of RF transmission properties of human tissues," *Advances in Radio Science*, vol. 4, pp. 357–360, sep 2006.

[7] H.-Z. T. Chen *et al.*, "A study of rf power attenuation in bio-tissues," *Journal of Medical and Biological Engineering*, vol. 24, pp. 141–146, 2004.

[8] E. Wen *et al.*, "Channel characterization of magnetic human body communication," *IEEE Transactions on Biomedical Engineering*, vol. 69, pp. 569–579, 2021.

[9] J.-C. Edelmann *et al.*, "Can you hear me now?: Challenges and benefits for connectivity of hearing aids and implants," *IEEE Microwave Magazine*, vol. 19, pp. 30–42, 2018.

[10] R. Gulati *et al.*, "Ultrasonic vs. magnetic resonance communication for mixed wearable and implanted devices," *Proc. of IEEE International Conf. on Communications (ICC)*, pp. 5304–5309, May 2022.

[11] G. A. Álvarez-Botero *et al.*, "Human body communication: Channel characterization issues," *IEEE Instrumentation Measurement Magazine*, vol. 22, pp. 48–53, 2019, an overview of different HBC technologies – Galvanic, Capacitive, Magnetic.

[12] W. J. Tomlinson *et al.*, "Comprehensive survey of galvanic coupling and alternative intra-body communication technologies," *IEEE Communications Surveys & Tutorials*, vol. 21, pp. 1145–1164, 2018.

[13] J. Park *et al.*, "Magnetic human body communication," in *2015 37th Annual International Conference of the IEEE Engineering in Medicine and Biology Society (EMBC)*. IEEE, 2015, pp. 1841–1844.

[14] R. K. Gulati *et al.*, "Characterization of magnetic communication through human body," *IEEE Consumer Communications and Networking Conference (CCNC)*, pp. 563–568, Jan 2022.

[15] S. Islam *et al.*, "Performance evaluation of magnetic resonance coupling method for intra-body network (ibnet)," *IEEE Transactions on Biomedical Engineering*, vol. 69, pp. 1901–1908, June 2022.

[16] F. Akasheh *et al.*, "Development of piezoelectric micromachined ultrasonic transducers," *Sensors and Actuators A: Physical*, vol. 111, pp. 275–287, 2004.

[17] A. Ibrahim *et al.*, "A comprehensive comparative study on inductive and ultrasonic wireless power transmission to biomedical implants," *IEEE sensors journal*, vol. 18, pp. 3813–3826, 2018.

[18] T. C. Chang *et al.*, "Design of Tunable Ultrasonic Receivers for Efficient Powering of Implantable Medical Devices With Reconfigurable Power Loads," *IEEE Transactions on Ultrasonics, Ferroelectrics, and Frequency Control*, vol. 63, pp. 1554–1562, Oct. 2016. [Online]. Available: http://ieeexplore.ieee.org/document/7562528/

[19] "Near field magnetic induction (nfmi): Dreams of wireless hearables," http://www.audioxpress.com/article/near-field-magnetic-induction-nfmi-dreams-of-wireless-hearables.

[20] R. Shukla *et al.*, "Skinnypower: enabling batteryless wearable sensors via intra-body power transfer," *Proceedings of the 17th Conference on Embedded Networked Sensor Systems*, 2019.

[21] A. Kim *et al.*, "An Ultrasonically Powered Implantable Microprobe for Electrolytic Ablation," *Scientific Reports*, vol. Under review, 2019.

[22] T. C. Chang *et al.*, "Design of Tunable Ultrasonic Receivers for Efficient Powering of Implantable Medical Devices With Reconfigurable Power Loads," *IEEE Transactions on Ultrasonics, Ferroelectrics, and Frequency Control*, vol. 63, pp. 1554–1562, Oct. 2016. [Online]. Available: http://ieeexplore.ieee.org/document/7562528/

[23] J. Park *et al.*, "A sub-10-pj/bit 5-mb/s magnetic human body communication transceiver," *IEEE Journal of Solid-State Circuits*, vol. 54, pp. 3031–3042, 2019.

[24] S. ZMT Zurich MedTech AG, Zurich, "Sim4life," https://zmt.swiss/sim4life/, Jan 2023.

[25] M. Masihpour *et al.*, "Cooperative relay in near field magnetic induction: A new technology for embedded medical communication systems," in *2010 Fifth International Conference on Broadband and Biomedical Communications (IB2Com)*. IEEE, 2010, pp. 1–6.

[26] I. Laakso *et al.*, "Evaluation of sar in a human body model due to wireless power transmission in the 10 mhz band," *Physics in medicine and biology*, vol. 57, pp. 4991–5002, 07 2012.

[27] T. Shimamoto *et al.*, "SAR evaluation in models of an adult and a child for magnetic field from wireless power transfer systems at 6.78 MHz," *Biomedical Physics Engineering Express*, vol. 2, p. 027001, mar 2016. [Online]. Available: https://doi.org/10.1088/2057-1976/2/2/027001

[28] K. Mizuno *et al.*, "In vitro evaluation of genotoxic effects under magnetic resonant coupling wireless power transfer," *International Journal of Environmental Research and Public Health*, vol. 12, pp. 3853–3863, Apr. 2015.

[29] "IEEE standard for safety levels with respect to human exposure to electric, magnetic, and electromagnetic fields, 0 hz to 300 GHz," 2019. [Online]. Available: https://doi.org/10.1109/ieeestd.2019.8859679

[30] I. C. on Non-Ionizing Radiation Protection *et al.*, "Guidelines for limiting exposure to electromagnetic fields (100 khz to 300 ghz)," *Health physics*, vol. 118, pp. 483–524, 2020.

[31] I. F. Akyildiz *et al.*, "Realizing underwater communication through magnetic induction," *IEEE Communications Magazine*, vol. 53, pp. 42–48, 2015.

[32] Z. Sun *et al.*, "Magnetic induction communications for wireless underground sensor networks," *IEEE Transactions on Antennas and Propagation*, vol. 58, pp. 2426–2435, 2010.

[33] N. Thilak *et al.*, "Near field magnetic induction communication in body area network," in *2012 International Conference on Devices, Circuits and Systems (ICDCS)*, 2012, pp. 124–125.

[34] H. Kim *et al.*, "Review of near-field wireless power and communication for biomedical applications," *IEEE Access*, vol. 5, pp. 21 264–21 285, 2017.

[35] K. Zhang *et al.*, "Near-field wireless power transfer to deep-tissue implants for biomedical applications," *IEEE Transactions on Antennas and Propagation*, vol. 68, pp. 1098–1106, 2019.

[36] R. Gulati *et al.*, "Experimental evaluation of a near-field magnetic induction based communication system," *Wireless Communications and Networking Conference, Marrakech, Morroco*, April 2019.

[37] A. Pal *et al.*, "Nfmi: Near field magnetic induction basedcommunication," *Elsevier Computer Networks*, Nov 2020.

[38] H. Guo *et al.*, "Channel modeling of MI underwater communication using tri-directional coil antenna," in *IEEE GLOBECOM*, 2015, pp. 1–6.

[39] C. A. Balanis, *Antenna Theory: Analysis and Design*. Wiley-Interscience, 2005.

[40] X. Tan *et al.*, "Environment-aware indoor localization using magnetic induction," in *IEEE GLOBECOM*, 2015, pp. 1–6.

[41] S. Gabriel *et al.*, "The dielectric properties of biological tissues: Ii. measurements in the frequency range 10 hz to 20 ghz," *Physics in medicine & biology*, vol. 41, p. 2251, 1996.

[42] N. Siauve *et al.*, "Electromagnetic fields and human body: a new challenge for the electromagnetic field computation," *COMPEL-The international journal for computation and mathematics in electrical and electronic engineering*, vol. 22, pp. 457–469, 2003.

[43] R. Cavallari *et al.*, "A survey on wireless body area networks: Technologies and design challenges," *IEEE Communications Surveys Tutorials*, vol. 16, pp. 1635–1657, Third 2014.

[44] B. Sigel, "A brief history of doppler ultrasound in the diagnosis of peripheral vascular disease," *Ultrasound in medicine & biology*, vol. 24, pp. 169–176, 1998.

[45] L. Galluccio *et al.*, "Challenges and implications of using ultrasonic communications in intra-body area networks," in *2012 9th Annual Conference on Wireless On-Demand Network Systems and Services (WONS)*. IEEE, 2012, pp. 182–189.

[46] K. Agarwal *et al.*, "Wireless power transfer strategies for implantable bioelectronics," *IEEE Reviews in Biomedical Engineering*, vol. 10, pp. 136–161, 2017.

[47] FDA, "Marketing clearance of diagnostic ultrasound systems and transducers: Guidance for industry and food and drug administration staff (fda-2017-d-5372)," *Rockville, MD: Center for Devices and Radiological Health, US Food and Drug Administration*, Jun. 2019.

[48] S. B. Barnett *et al.*, "International recommendations and guidelines for the safe use of diagnostic ultrasound in medicine," *Ultrasound in medicine & biology*, vol. 26, pp. 355–366, 2000.

[49] P. M. Shankar, "A general statistical model for ultrasonic backscattering from tissues," *IEEE transactions on ultrasonics, ferroelectrics, and frequency control*, vol. 47, pp. 727–736, 2000.

[50] A. C. Saavedra *et al.*, "Measurement of surface acoustic waves in high-frequency ultrasound: Preliminary results," in *2017 39th Annual International Conference of the IEEE Engineering in Medicine and Biology Society (EMBC)*, 2017, pp. 3000–3003.

[51] M. D. Maas, "Open-source electromagnetic simulation: Fdtd, fem, mom," https://www.matecdev.com/posts/differences-fdtd-fem-mom.html, Aug 2021.

[52] K.-W. Yang *et al.*, "Challenges in scaling down of free-floating implantable neural interfaces to millimeter scale," *IEEE Access*, vol. 8, pp. 133 295–133 320, 2020.

[53] C. Han *et al.*, "The wireless power transmission on the wrist-to-forehead path based on the body channel," *JOURNAL OF BEIJING INSTITUTE OF TECHNOLOGY*, vol. 31, pp. 91–100, 2022.